



HAL
open science

Field nano-localization of gas bubble production from water electrolysis

Z. Hammadi, R. Morin, Juan Olives

► **To cite this version:**

Z. Hammadi, R. Morin, Juan Olives. Field nano-localization of gas bubble production from water electrolysis. Applied Physics Letters, 2013, 103 (22), pp.223106. 10.1063/1.4836095 . hal-02089349

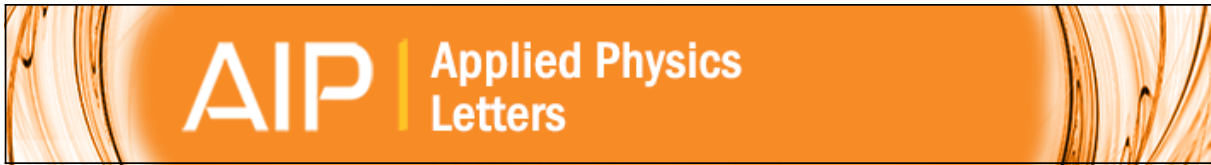
HAL Id: hal-02089349

<https://hal.science/hal-02089349>

Submitted on 25 Apr 2019

HAL is a multi-disciplinary open access archive for the deposit and dissemination of scientific research documents, whether they are published or not. The documents may come from teaching and research institutions in France or abroad, or from public or private research centers.

L'archive ouverte pluridisciplinaire **HAL**, est destinée au dépôt et à la diffusion de documents scientifiques de niveau recherche, publiés ou non, émanant des établissements d'enseignement et de recherche français ou étrangers, des laboratoires publics ou privés.



Field nano-localization of gas bubble production from water electrolysis

Z. Hammadi, R. Morin, and J. Olives

Citation: [Applied Physics Letters](#) **103**, 223106 (2013); doi: 10.1063/1.4836095

View online: <http://dx.doi.org/10.1063/1.4836095>

View Table of Contents: <http://scitation.aip.org/content/aip/journal/apl/103/22?ver=pdfcov>

Published by the [AIP Publishing](#)



Re-register for Table of Content Alerts

Create a profile.



Sign up today!



Field nano-localization of gas bubble production from water electrolysis

Z. Hammadi, R. Morin,^{a)} and J. Olives

CINaM, CNRS, Aix-Marseille University, Campus de Luminy, Case 913, 13288 Marseille Cedex 9, France

(Received 6 September 2013; accepted 10 November 2013; published online 26 November 2013)

Using a tip shaped electrode and ac voltages, we show that the production of micro bubbles of gas from water electrolysis is localized at the tip apex inside a domain in the voltage frequency phase space. A model taking into account the electrode shape and dimensions explains these results which suggest a field effect control of the electrolysis reaction rate at a nanometer scale. © 2013 AIP Publishing LLC. [<http://dx.doi.org/10.1063/1.4836095>]

Gas bubbles appear in various natural or artificial phenomena such as the formation and the stability of nanobubbles at the surface of solids¹ or the properties of bubble phononic crystals.² They are also the object of several concerns in medicine, such as the behaviour of microbubble contrast agent³ or the dynamics of microbubbles in gas embolotherapy,⁴ and in technology such as the spark assisted chemical engraving of glass⁵ or the role of bubbles in the electroflotation process.⁶ As a consequence, various mechanisms to produce bubbles using heat,⁷ light,⁸ ultrasounds,⁹ capillary flow,¹⁰ or electrolysis¹¹ as well as various sources able to deliver well defined bubbles^{12–15} have been the object of recent studies especially in the microfluidics context. Here, we focus on the bubble production mechanism by water electrolysis and on the realization of a point source of bubbles based on this mechanism.

Production of gas bubbles by water electrolysis in an acidic or alkaline solution is a fundamental process in electrochemistry. Involved electrochemical reactions are oxidation at the anode with O₂ evolution ($2\text{H}_2\text{O} \rightarrow 4\text{H}^+ + 4\text{e}^- + \text{O}_2$ or $4\text{OH}^- \rightarrow 2\text{H}_2\text{O} + 4\text{e}^- + \text{O}_2$) and reduction at the cathode with H₂ evolution ($2\text{H}^+ + 2\text{e}^- \rightarrow \text{H}_2$ or $2\text{H}_2\text{O} + 2\text{e}^- \rightarrow \text{H}_2 + 2\text{OH}^-$) depending on voltage and availability of reactants. An ac voltage sequentially reverses the role of electrodes and the nature of the produced gas. However, this simple molecular view does not describe many features observed in a real experiment. Using optical microscopy, for instance, one observes that gas bubbles are produced at some definite but apparently unpredictable locations at the surface of electrodes (Fig. 1(a)). This suggests the existence of sites on the surface where the reaction rate is locally high, and that these sites likely correspond to chemical or morphological heterogeneities. Since this is observed even on high purity and highly polished electrodes, it is expected that the typical scale characterizing these heterogeneities is beyond the optical microscope resolution, i.e., the nanometer scale.

Here, we show the localization of the production of bubbles on a single site of a macroscopic electrode, the apex of a tip shaped electrode (Fig. 1(b)), using an ac electrolysis voltage. We show that this localization takes place inside a domain in the voltage frequency phase space and explain these results by a simple model. These results strongly support the

control of the localization of an electrochemical reaction on an even equipotential electrode.

The localization on one single site provides several specific advantages. First, it reduces pertinent parameters to those characterizing the site (Fig. 1(c)).¹⁶ Second, bubbles are produced one after the other¹⁶ which makes possible to study a single bubble with poor spatial resolution methods like acoustic probes, for instance. Third, high spatial resolution techniques focused on a single site combined with time control of voltage, and high speed microscopy technique can be used to unravel the bubble formation.

The experimental setup is shown in Fig. 2. We carried out experiments with tip shaped electrodes made of W, Au, and Pt round shaped counter electrodes (C and Pt), and various electrolytes (NaCl, HCL, and H₂SO₄) at different concentrations. The tip is first etched from a wire, and then the wire is bent to form a hook. Then, this tip and the counter electrodes are immersed in a transparent tank containing the electrolyte. Voltage on the tip is applied from an ac voltage generator (Agilent 33120 A) via a high voltage high speed amplifier (Falco System WMA-300, 150 V maximum output, 2000 V/μs slew rate). A binocular (up to X 50) and an optical digital microscope (up to X 220) are used to observe bubbles and record pictures.

At a fixed ac frequency, increasing the tip voltage first triggers the appearance of one single string of bubbles from one site on the tip apex (voltage V_a). Increasing the voltage keeps one single string of bubbles up to V_s, where bubbles appear from many sites on the tip shank. Up to a frequency f_{loc}, V_a ≈ V_s. Above f_{loc}, V_a is significantly distinct from V_s. V_a is easy to determine since it corresponds to the appearance of bubbles from a single site on the apex. V_s is also easy to determine for tips with small shank angle (a few degrees) because as soon as bubbles appear on the shank, they quickly appear on a large part of the shank surface. For

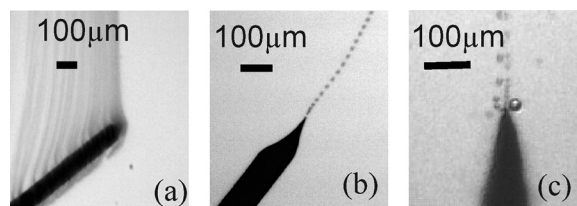


FIG. 1. (a) Usual delocalized bubble production. (b) Localized on a single site. (c) Localized on 3 sites with different bubble production characteristics.

^{a)}morin@cinam.univ-mrs.fr

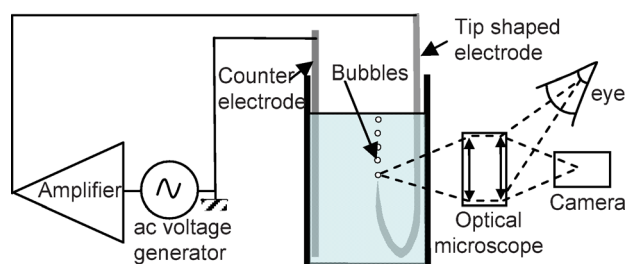


FIG. 2. Scheme of the experimental setup.

large shank angles (more than 20°), bubbles appear more progressively on the shank making V_s determination more arbitrary. As the frequency is gradually decreased, bubbles start to appear after a longer and longer time making V_a and V_s determinations more difficult, and their values may be overestimated. For a given tip, V_a and V_s determinations are reliable as long as too high voltages are not applied to the tip. Such high voltages cause irreversible damage to the tip, a dark aspect of its surface or a growth of material onto it. Using NaCl or HCl electrolytes or W or Au tips also leads to rapid damages to the tip. However, for Pt tips, Pt counter electrodes, and H_2SO_4 at low concentration, the bubble production at the apex of the tip is stable for days at moderate voltages. At higher voltages, one can still observe bubbles and measure V_a and V_s before the tip changes.

Fig. 3 shows results (V_a and V_s vs frequency) for a Pt tip, a Pt counter electrode and H_2SO_4 at 10^{-4} mol/l.

Because the localization of bubble production is obtained using tip shaped electrodes, we studied the influence of this shape, performing experiments with 22 Pt tips, observed by optical microscopy (and some of them by electron microscopy). Studied tip shapes were small shank angle and small apex radius (S shape) and large shank angle and large apex radius (L shape) (Fig. 4). We restrict measurements to V_a vs frequency f . From these measurements, we extract (Table I) the low frequency voltage $V_0 = V_a$ ($f = 1$ Hz) and the frequency f_c from which V_a strongly increases with frequency. V_0 and f_c dependences with H_2SO_4 concentration are also reported in Table I.

Obviously an explanation of our experimental results has to take into account the high curvature at the tip apex

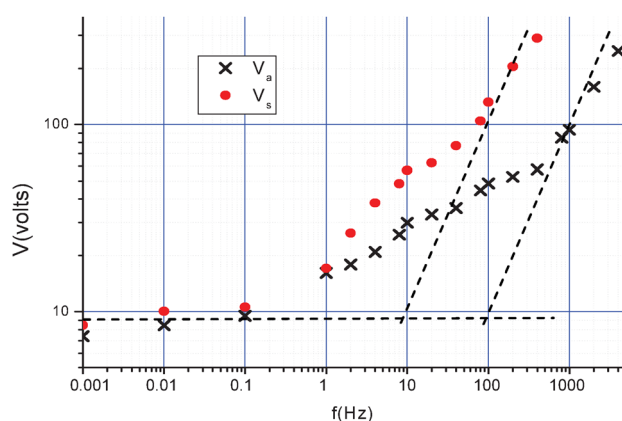


FIG. 3. Onset voltages (volt peak to peak) vs frequency to observe bubbles: (\times , V_a) at the tip apex (\bullet , V_s) along the shank Pt tip, Pt counter electrode, 10^{-4} mol H_2SO_4 /l.

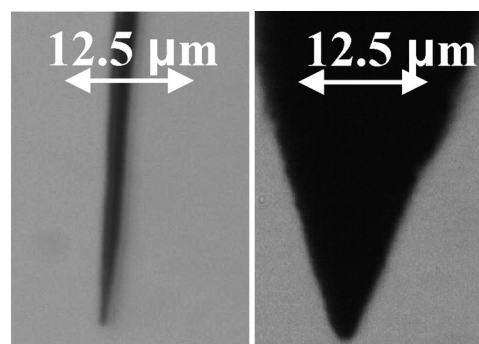


FIG. 4. Optical micrograph of S (small shank angle and small apex radius) type (left) and L (large shank angle and large apex radius) type (right) tip shapes.

and ignore details of the reaction since results are obtained for most metal tip-electrolyte combinations we used. We assume in a first approximation that at any point of the tip surface bubbles appear as soon as the rate of the most limiting electrochemical reaction at this point reaches a threshold value. This rate is proportional to the rate of charge transfer through the electrode/electrolyte interface. This interface is known to be a few water layers thick.^{17–20} Let us assume that this layer constitutes a uniform (thickness e both at the apex and along the shank of the tip) dielectric (permittivity ϵ) layer, and that the charge transfer rate is controlled by the voltage v applied to this dielectric layer.^{21–23} Because of the relatively high voltage, we suspect tunnelling by field effect through this layer.^{24,25} Beyond this layer, the electrolyte is considered as a conductor with conductivity γ and permittivity ϵ . V is the ac voltage applied to the tip relative to the counter electrode.

Hereafter, we show that the ac voltage v on the dielectric layer depends on position (apex or shank) along the tip surface, and this explains the observed experiments.

First, a qualitative explanation: if the applied voltage V is slowly changed, the current in the conductor supplies charges on the dielectric/conductor interface in order to keep the same potential in the conductor. Therefore, $v = V$ at any position along the tip surface. If the applied voltage V is abruptly changed, a short time later charge supply to the dielectric/conductor interface is too small to cancel the field in the conductor so that a voltage drop is present in the conductor and $v < V$. However, the field in the conductor is not uniform for a tip shaped electrode; in particular, at the dielectric/conductor interface, it is larger at the tip apex than along the shank. Since charge supply to this interface is proportional to this field, charge density at this interface increases faster at the tip apex than along the shank. Consequently, v is higher at the tip apex than along the shank.

Analytical calculations illustrate this behaviour for simple electrode geometries, e.g., two concentric spherical electrodes or two coaxial cylindrical electrodes (radii r and R for the tip electrode and the counter electrode, respectively). For a periodic voltage V at frequency f , solving Maxwell equations for these geometries¹⁶ gives

$$V = v(1 + jf/f_1)/(1 + jf/f_0),$$

TABLE I. Results obtained from experiments on 11 tips with small shank angles and small apex radius (type S) and 11 tips with large shank angles and large apex radius (Type L): V_0 is the minimum voltage to observe bubbles at 1 Hz and f_c is the frequency from which the voltage V_a to observe bubbles only at the tip apex strongly increases with frequency.

H_2SO_4 concentration	10^{-5} mol/l	10^{-4} mol/l	10^{-3} mol/l	10^{-2} mol/l
Type S (see Fig. 4)		$10 \text{ V} < V_0 < 25 \text{ V}$ $100 \text{ Hz} < f_c < 1 \text{ kHz}$	$6 \text{ V} < V_0 < 8 \text{ V}$ $1 \text{ kHz} < f_c < 10 \text{ kHz}$	$3 \text{ V} < V_0 < 4 \text{ V}$ $f_c > 10 \text{ kHz}$
Type L (see Fig. 4)	$14 \text{ V} < V_0 < 25 \text{ V}$ $10 \text{ Hz} < f_c < 100 \text{ Hz}$	$10 \text{ V} < V_0 < 12 \text{ V}$ $100 \text{ Hz} < f_c < 1 \text{ kHz}$	$4 \text{ V} < V_0 < 5 \text{ V}$ $f_c > 1 \text{ kHz}$	

where $j^2 = -1$, $f_0 = \gamma/(2\pi\epsilon)$, and $f_1 = f_0/\alpha$, where $\alpha = 1 + r/e$ [R - (r + e)]/R for the spherical geometry and $\alpha = 1 + \text{Ln}[R/(r + e)]/\text{Ln}(1 + e/r)$ for the cylindrical geometry.

In a crude approximation, the field at the apex of the tip of radius r is estimated from the field in the sphere model with an inner sphere radius r (the field at the apex of a tip of radius r at potential V placed at a large distance from a counter electrode is $\sim V/(5r)$)^{26,27} and the field at the shank of the tip from the field in the cylinder model with an inner cylinder radius r ; the distance to the counter electrode is estimated to be the outer electrode diameter in both models. e , r , and R dimensions are, respectively, nanometric, micrometric, and millimetric, so that $e \ll r \ll R$. Since bubbles are produced above a threshold value of the reaction rate, they are produced for $v > v_0$ thus for

$$V > V_a = v_0|1 + jf/f_a|/|1 + jf/f_0| \quad (1)$$

with $f_a \approx f_0/(1 + r/e)$

at the tip apex and

$$V < V_s = v_0|1 + jf/f_s|/|1 + jf/f_0| \quad (2)$$

with $f_s \approx f_0/[(1 + r/e) \text{Ln}(R/r)]$

along the tip shank. In a Bode representation ($\log |V|$ vs $\log f$), the bubble production is described in Fig. 5. The bubbles are produced only at the tip apex for voltages V between V_s and V_a depending on frequency.

The experimental results reported in Fig. 3 agree with this model, which predicts at low frequency a direct transition

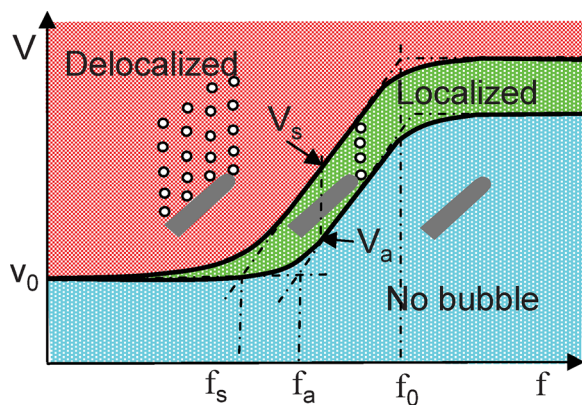


FIG. 5. Frequency-voltage (logarithmic) diagram indicating the characteristics of bubble production (based on the sphere/cylinder model for the determination of the field). The bubble production is absent at low voltage and delocalized on the whole surface (shank and apex) of the tip at high voltage. The bubble production is localized at the tip apex between V_a and V_s curves.

from a “no bubble” production regime to a “delocalized” one, and at finite frequency a transition between these regimes via a tip-apex “localized” one. The high frequency behaviour ($f > f_0$) is not observed because of both amplifier voltage limitation and changes on the tip at high voltage. Slope 1 linear fitting of the high frequency V_s and V_a plots leads to $f_s \approx 10 \text{ Hz}$ and $f_a \approx 100 \text{ Hz}$.

f_0 is determined from the conductivity $\gamma = 0.0078 \text{ S/m}$ of the electrolyte ($10^{-4} \text{ H}_2\text{SO}_4 \text{ mol/l}$) and the relative dielectric permittivity of water $\epsilon_r = 80$ (Ref. 28) giving $f_0 = 1.7 \text{ MHz}$. Therefore, experimental values $f_s \approx 10 \text{ Hz}$ and $f_a \approx 100 \text{ Hz}$, and Eqs. (1) and (2) lead to

$$r/e \approx f_0/f_a - 1 \approx 1.7 \times 10^4$$

and $R/r = \exp[f_a/f_s] \approx 2.2 \times 10^4$.

As previously mentioned, since the field at the apex of a tip is roughly 5 times less than the field of a sphere of same radius, $(f_0/f_a - 1)$ overestimates r/e . A better estimate is $r/e \approx (f_0/f_a - 1)/5 \approx 3.4 \times 10^3$. Taking into account the crudeness of our model these values agree reasonably well with the thickness of the interface $e \approx 0.3 \text{ nm}$,¹⁹ the observed mean radius of curvature of the used Pt tips $r \approx 1 \mu\text{m}$, and the macroscopic distance between the tip and the counter electrode is $R \approx 10 \text{ mm}$.

The model predicts that f_s and f_a are proportional to the conductivity γ and therefore to the acid concentration. This agrees with the influence of the acid concentration on the frequency f_c reported in Table I. At low frequency, the model predicts that $V_a \approx V_s \approx v_0$ independent of frequency and acid concentration (i.e., γ). Experiments actually show that $V_a \approx V_s$ at low frequency, but that this value increases with frequency and decreases with concentration (see Table I for V_0). An additional ohmic effect related to a saturation effect of the current density, not included in our model, might be responsible for this behaviour.

Among the assumptions made, i.e., (i) the description of the electrolyte as a serial circuit made of a dielectric layer and a bulk conductor, (ii) the field and frequency independence of the permittivity ϵ , of the thickness e and of the conductivity γ , (iii) the determination of the field value at the tip apex and at the tip shank obtained from a simplified geometrical description, and (iv) finally, the assumption that the bubble production rate only depends on the local electrochemical reaction rate, the later is the most questionable. A more realistic view is that the production (nucleation and growth) of bubbles is governed by the concentration of dissolved gas.^{29,30} But this concentration does not only result from the gas production but also from diffusion of this gas.

Because of diffusion, the distance which governs the gas concentration decrease from the apex is $\sim(D/f)^{1/2}$. Therefore, tip and shank are distinguishable if this distance is smaller than the tip radius ($\sim 1 \mu\text{m}$). For H_2 , $D \approx 5 \times 10^{-9} \text{ m}^2/\text{s}$ so that tip and shank are distinguishable for $f > 5 \text{ kHz}$. We expect that this is why V_a and V_s are not proportional to frequency below 1 kHz (Fig. 3). Apart from diffusion, convective flow generated by density gradient related to gas concentration difference as well as bubble growth and bubble escape also contribute to variations of gas concentration. Presently, we do not have a simple theoretical description of these processes.

With regard to the control of the localization of a chemical reaction at a nanometer scale obtained between a tip and a nearby surface using near field microscopy techniques,^{31–34} the electrolytic reaction is here localized at the tip apex of a tip shaped electrode but far away from the counter electrode. This localization results from the localization of the electric field which itself results from the use of both a tip shaped electrode and appropriate voltage and frequency values. So, a point source of bubbles is built, which provides a very unique environment, widely open to various probes, to study bubble properties.

We thank Serge Mensah and Younes Achaoui for discussions and Marjorie Sweetko for English language revision. This work was supported by ANR through the “SmartUS” Project.

¹J. H. Weijss and D. Lohse, *Phys. Rev. Lett.* **110**, 054501 (2013).

²V. Leroy, A. Bretagne, M. Fink, H. Willaime, P. Tabeling, and A. Tourin, *Appl. Phys. Lett.* **95**, 171904 (2009).

³S. H. Bloch, M. Wan, P. A. Dayton, and K. W. Ferrara, *Appl. Phys. Lett.* **84**(4), 631–633 (2004).

⁴A. Qamar, Z. Z. Wong, J. B. Fowlkes, and J. L. Bull, *Appl. Phys. Lett.* **96**, 143702 (2010).

⁵R. El-Haddad and R. Wuethrich, *J. Appl. Electrochem.* **40**(10), 1853–1858 (2010).

⁶M. M. Emamjomeh and M. Sivakumar, *J. Environ. Manage.* **90**(5), 1663–1679 (2009).

⁷V. S. Nikolayev, D. Chatain, Y. Garrabos, and D. Beysens, *Phys. Rev. Lett.* **97**, 184503 (2006).

⁸B. C. Knott, J. L. LaRue, A. M. Wodtke, M. F. Doherty, and B. Peters, *J. Chem. Phys.* **134**, 171102 (2011).

⁹K. B. Bader, J. Mobley, C. C. Church, and D. F. Gaitan, *J. Acoust. Soc. Am.* **132**(2), 728–737 (2012).

¹⁰G. F. Christopher and S. L. Anna, *J. Phys. D: Appl. Phys.* **40**, R319–R336 (2007).

¹¹B. C. Donose, F. Harnisch, and E. Taran, *Electrochem. Commun.* **24**, 21–24 (2012).

¹²A. M. Ganan-Calvo and J. M. Gordillo, *Phys. Rev. Lett.* **87**, 274501 (2001).

¹³P. Garstecki, P. I. Gitlin, W. DiLuzio, G. M. Whitesides, E. Kumacheva, and H. A. Stone, *Appl. Phys. Lett.* **85**(13), 2649–2651 (2004).

¹⁴S. Lee, W. Sutomo, C. Liu, and E. Loth, *Int. J. Multiphase Flow* **31**, 706–722 (2005).

¹⁵M. Stoffel, S. Wahl, E. Lorenceau, R. Höhler, B. Mercier, and D. E. Angelescu, *Phys. Rev. Lett.* **108**, 198302 (2012).

¹⁶See supplementary material at <http://dx.doi.org/10.1063/1.4836095> for bubble production from 3 sites with different characteristics (large bubbles are randomly produced); periodic production of bubbles from a single site (9V, 1Hz, sharp tip, $\times 5$ magnification); and solution of Maxwell equations for spherical and cylindrical geometries.

¹⁷X. Xia and M. L. Berkowitz, *Phys. Rev. Lett.* **74**(16), 3193–3196 (1995).

¹⁸R. Guidelli and W. Schmickler, *Electrochim. Acta* **45**, 2317–2338 (2000).

¹⁹J. Rossmeißl, E. Skulason, M. E. Bjorketun, V. Tripkovic, and J. K. Nørskov, *Chem. Phys. Lett.* **466**(1–3), 68–71 (2008).

²⁰M. Osawa, M. Tsushima, H. Mogami, G. Samjeské, and A. Yamakata, *J. Phys. Chem. C* **112**(11), 4248–4256 (2008).

²¹T. Nagy, D. Henderson, and D. Boda, *J. Phys. Chem. B* **115**(39), 11409–11419 (2011).

²²D. Boda, D. Henderson, B. Eisenberg, and D. Gillespie, *J. Chem. Phys.* **135**(6), 064105 (2011).

²³J. K. Nørskov, J. Rossmeißl, A. Logadottir, L. Lindqvist, J. R. Kitchin, T. Bligaard, and H. Jónsson, *J. Phys. Chem. B* **108**, 17886–17892 (2004).

²⁴M. Galperin and A. Nitzan, *J. Phys. Chem. A* **106**(45), 10790–10796 (2002).

²⁵Z. Hammadi, M. Descoins, E. Salançon, and R. Morin, *Appl. Phys. Lett.* **101**, 243110 (2012).

²⁶R. Gomer, *Field Emission and Field Ionization* (Harvard University Press, Cambridge, 1961).

²⁷G. S. Gipson and H. C. Eaton, *J. Appl. Phys.* **51**(10), 5537 (1980).

²⁸In Ref. 21, authors show that $\varepsilon \approx 40$ would be more appropriate which does not change our conclusions.

²⁹P. Maciel, T. Nierhaus, S. Van Damme, H. Van Parys, J. Deconinck, and A. Hubin, *Electrochem. Commun.* **11**, 875–877 (2009).

³⁰H. Vogt, *Electrochim. Acta* **56**, 1409–1416 (2011).

³¹N. J. Tao, C. Z. Li, and H. X. He, *J. Electroanal. Chem.* **492**, 81–93 (2000).

³²R. Schuster, V. Kirchner, P. Allongue, and G. Ertl, *Science* **289**, 98 (2000).

³³O. de Abril, A. Gündel, F. Maroun, P. Allongue, and R. Schuster, *Nanotechnology* **19**, 325301 (2008).

³⁴T. Albrecht, *Nature Commun.* **3**, 829 (2012).